CARBON letters

Note

Carbon Letters Vol. 21, 111-115 (2017)

The effects of carbon coating onto graphite filler on the structure and properties of carbon foams

Ji-Hyun Kim, Do Young Kim and Young-Seak Lee*

Department of Chemical Engineering and Applied Chemistry, Chungnam National University, Daejeon 34134, Korea

Article Info

Received 19 October 2016
Accepted 5 November 2016

***Corresponding Author**
E-mail: youngslee@cnu.ac.kr
Tel: +82-42-821-7007

Open Access

DOI: http://dx.doi.org/10.5714/CL.2017.21.111

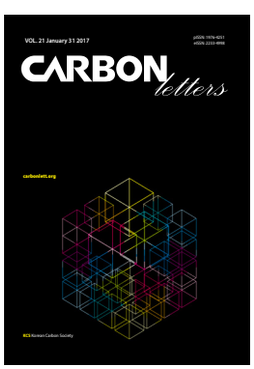

http://carbonlett.org

pISSN: 1976-4251
eISSN: 2233-4998

Carbon foams (CFms) are of crucial importance in electrical and mechanical devices due to their high thermal conductivity used for eliminating high heat flow and maintaining low temperatures [1]. The most common CFms are types of aluminum alloys, copper and diamond. However, the mechanical properties of metal-based heat sink materials are difficult to control at temperatures over 550°C [2,3]. Thus, CFms are actively investigated as heat sink materials because of their good properties, such as high thermal stability, high thermal/electrical conductivity, low density, high porosity and high specific surface area [4,5]. CFms are suitable materials for applications in phase-change materials, such as in latent heat thermal energy storage and lithium-ion batteries [6-9].

CFms are prepared from thermoplastic graphitizable precursors, such as petroleum-derived, coal-derived and mesophase pitch (MP). In particular, MP has been widely used as an appropriate precursor for high-performance carbon materials due to its attractive properties, i.e., high coke yield, low softening point, and high fluidity [10]. Previous processes used a blowing technique, or pressure release, to produce foam from MP. These manufacturing techniques have many disadvantages: the volume fraction of generated cells cannot be precisely controlled, and controlling the shape and distribution of cells is difficult, if not impossible [11]. To better control and tailor the structure of such foams, polymer template methods are actively being researched. Hydrogel template methods are suitable for preparing high-strength CFms due to their large quantities of carbon precursors and the pressure generated through hydrogel shrinkage via heat treatment [10,12]. However, their mechanical strengths are low because of their high porosities.

One method for improving the mechanical strength of CFms is adding fillers with a high mechanical strength. Several additives have been used as fillers, including carbon nanofibers, short carbon fibers, graphite and graphene nanosheets [13-22]. In particular, graphite has beneficial properties that include high lubricating ability, heat resistance, corrosion resistance and thermal/electrical conductivity. It has been widely applied in various fields as a highly functional component with efficient properties. Additionally, the theoretical thermal conductivity of graphite is high, with values ranging from 3000 to 5000 W/mK, and its mechanical strength is 1100 GPa [23,24]. The thermal/mechanical properties of CFms could be improved by the addition of carbon nanofillers with good thermal/mechanical properties through the formation of network structures comprising CFms and carbon nanofillers. Furthermore, carbon nanofillers can be carbon-coated (C-coated) to improve the interfacial bonding with metal. For example, Katzman [25] showed that carbon fibers could be C-coated using amorphous pitch to improve the interfacial bonding with metal oxide and prepare a carbon-fiber-reinforced metal-matrix composite with a relatively high modulus. Thus, in this study, a graphite filler was C-coated to improve the structure and properties of CFms. The graphite was C-coated using different concentrations of quinolone-insoluble content (QI)-free MP. The thermal/mechanical properties of the CFms containing the C-coated graphite were investigated in terms of improving the interfacial adhesion between the CFms and the C-coated graphite.

MP with a softening point of 275–295°C, a QI of 75–87% and a quinolone-soluble content of 13–25% was prepared from coal tar pitch [26], which was used as a precursor for preparing the CFms. The QI-free MP was used to C-coat the graphite. Graphite (≤ 20 μm; Sigma-Aldrich, USA) was used as a filler in the CFms. Poly(vinyl alcohol)/acrylic acid

(PVA-AAc)-based hydrogels were prepared using the same materials [12].

To prepare the C-coated graphite, graphite (900 mg) and QI-free MP (50, 100, 200, and 300 mg) were placed in tetrahydrofuran (100 mL) and stirred for 24 h, resulting in QI-free MP concentrations of 0.5, 1.0, 2.0, and 3.0 wt%, respectively. After stirring for 24 h, the solvent was evaporated at 120°C, and the material was dried at 100°C for 12 h. The obtained MP-coated graphite was carbonized at 1000°C for 1 h with a heating rate of 5°C/min. The acquired C-coated graphite samples were labeled C0.5G, C1.0G, C2.0G and C3.0G, respectively. The un-coated graphite was labeled C0.0G. After preparing the gel solution [12], the C-coated graphite (0.078 g, 0.3 wt% per the weight of the stabilized MP) was added to the prepared gel solution and stirred for 1 h to disperse the C-coated graphite in the gel solution. The MP was stabilized at 280°C for 2 h with a heating rate of 1°C/min in an air atmosphere for a high carbon yield. The stabilized MP (26 g) was added to the gel solution with C-coated graphite and stirred for 1 h to mix the stabilized MP and C-doped graphite uniformly. The obtained mixture was heat-treated at 60°C for 9 h and dried at 140°C for 13 h. The dried hydrogel containing the MP and the C-coated graphite was carbonized at 1000°C for 1 h with a heating rate of 5°C/min in a nitrogen atmosphere. The obtained CFms were labeled CFm, CFm-C0.0G, CFm-C0.5G, CFm-C1.0G, CFm-C2.0G and CFm-C3.0G, respectively.

The surface morphologies and cell sizes of the CFms containing C-coated graphite were examined using field-emission scanning electron microscopy (S-8230; Hitachi, Japan) to investigate the interfacial binding between the CFms and the C-coated graphite. The crystallinity of the prepared CFms was examined using Raman spectroscopy (RM 1000-InVia; Renishaw, Korea) with an excitation power of 10 mW at 514 nm and X-ray diffraction (XRD; D/MAX-2200 Ultima/PC, Rigaku, Japan). The compressive strengths of at least five prepared CFm specimens were analyzed using a MicroMaterial Tester (Instron 5848, 500 N; Instron, USA) with a sample size of 6 × 6 × 6 mm^3. The thermal conductivities of at least three prepared CFm specimens were analyzed at 25°C using a xenon flash diffusivity technique in the axial direction with samples 12.5 × 12.5 × 3 mm^3 in size (ASTM E1461). The compressive strength and thermal conductivity of the selected samples were analyzed.

The graphite was C-coated with different QI-free MP concentrations to improve the interfacial adhesion between the C-coated graphite and the CFms, as shown in Fig. 1. QI-free MP was used as the C-coating material because it possesses several characteristics, including isotropic properties and a high carbonization yield, and it can uniformly coat carbon materials [6]. As a reference, Fig. 1a shows the smooth surface morphology of the graphite material. The surface morphologies of the C-coated graphite are shown in Fig. 1b-d. The C-coated surface roughness of the graphite increased with increasing MP concentration. The graphite was C-coated with MP in a carbon sheet shape, the sheet size of which grew with increasing MP concentration.

The coating thickness of the C-coated graphite was analyzed using particle size distribution, as shown in Fig. 2a. The un-coated graphite, C0.0G, had a particle size distribution ranging from

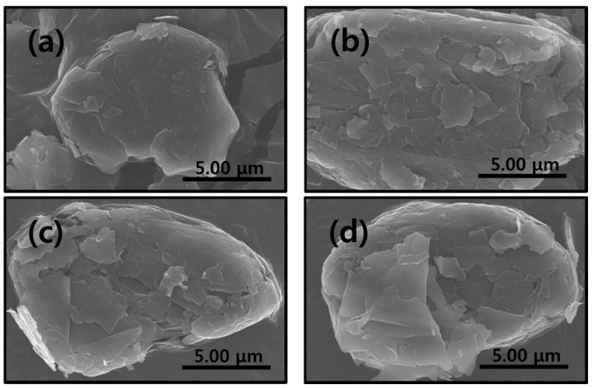

Fig. 1. Surface morphologies of the carbon-coated graphite: (a) C0.0G, (b) C0.5G, (c) C1.0G and, (d) C2.0G.

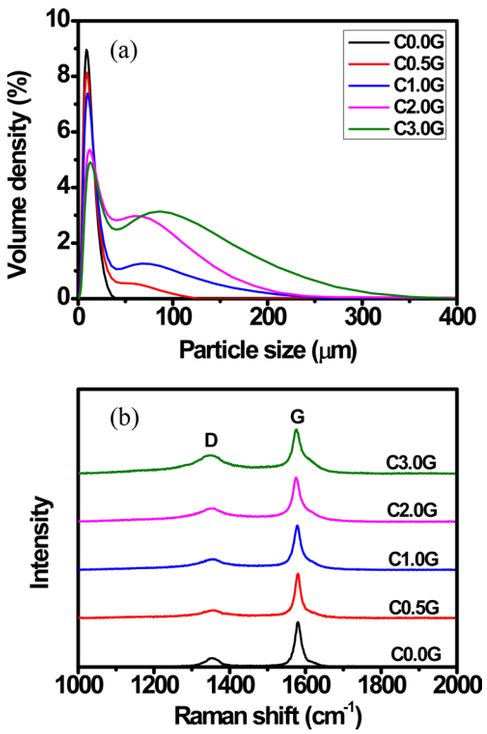

Fig. 2. (a) Particle size distributions and (b) Raman analysis of carbon-coated graphite.

0.872 to 35.3 μm, and the average particle size was 8.68 μm. The range of the C-coated graphite particle size distributions increased with increasing MP concentration, as demonstrated by the following increasing average particle sizes: 58.90, 66.90, 66.90, and 86.40 μm for C0.5G, C1.0G, C2.0G, and C3.0G, respectively. Additionally, the corresponding average C-coating thicknesses were approximately 50.22, 58.22, 58.22, and 77.72 μm, respectively. The crystalline defects of the C-coated graphite were analyzed by Raman spectroscopy, as shown in Fig. 2b. The crystalline peaks of the carbon materials were observed at the G and D peaks of the Raman spectrum, which were at 1580 and 1350 cm^{-1}, respectively. G-mode was analyzed by the E_{2g}

vibrations of graphitic structures (sp^2) at 1580 cm^{-1}, which were attributed to the vibrations of C-coated graphite. D-mode was analyzed by the A_{1g} vibrations of defective sp^2 structures at 1350 cm^{-1}, which were attributed to the vibrations of non-graphitic structures in the C-coated graphite [27]. The crystalline structure of C-coated graphite was confirmed using the D to G peak intensity ratio (I_D/I_G), which were indicated to be 0.18, 0.20, 0.24, 0.30, and 0.42 for C0.0G, C0.5G, C1.0G, C2.0G, and C3.0G, respectively. The I_D/I_G ratios of the C-coated graphite increased with increasing amounts of non-graphitic structures in the C-coatings.

The cell sizes and the interfacial binding between the CFms and the C-coated graphite were analyzed by scanning electron microscopy, as shown in Fig. 3. The cell sizes were indicated to be 293 ± 97, 332 ± 143, 212 ± 86, 319 ± 56, 352 ± 73, and 509 ± 180 μm for CFm, CFm-C0.0G, CFm-C0.5G, CFm-C1.0G, CFm-C2.0G, and CFm-C3.0G, respectively. The cell size of the CFm-C0.0G sample increased compared with that of CFm because the graphite powder was initially incorporated into the cell walls of the CFms. After adding C-coated graphite into the CFms, the cell sizes of the CFms containing C-coated graphite first decreased and then increased with increasing amounts of graphite C-coating. We attributed the reduction in cell size to increased interfacial binding between the CFms and the C-coated graphite and the subsequently increased cell size to the increased C-coated graphite particle sizes in the CFms due to their lower surface area by interpolation [23]. The inserted images in the bottom left of Fig. 3a and b show the surface morphology of the uniform CFms obtained, while CFm-0.0G was non-uniform. The inserted images in the bottom left of Fig. 3c-f illustrate the surface morphologies of the CFms containing C-coated graphite, which show increasing interfacial binding between the CFms and C-coated graphite with increasing amounts of C-coating on the graphite. The crystalline defects of the CFms containing C-coated graphite were analyzed by Raman spectroscopy. The I_D/I_G ratios of each peak intensity were indicated to be 1.03, 0.94, 0.89, 0.93, 0.93, and 0.94 for CFm, CFm-C0.0G, CFm-C0.5G, CFm-C1.0G, CFm-C2.0G, and CFm-C3.0G, respectively, as shown in Table 1. The I_D/I_G ratio of CFm-C0.0G was lower than that of the CFms due to the addition of graphite with highly graphitic structures. The I_D/I_G ratios of the CFms containing C-coated graphite decreased and then slightly increased with increasing amounts of graphite C-coating. The I_D/I_G reduction was attributed to improvement in interfacial binding between the CFms and the C-coated graphite filler with reduced crystalline defects. Additionally, the crystalline structures of the CFms containing C-coated graphite were examined in detail by XRD. Table 1 shows the interlayer spacing and crystalline size of the CFms containing C-coated graphite filler. CFm alone showed an interlayer spacing of 0.3553 nm and a crystalline size of 1.701 nm, respectively. CFm-C0.0G had an interlayer spacing of 0.3568 nm and a crystalline size of 2.142 nm. The interlayer spacings of the CFms containing C-coated graphite showed no significant differences. However, the crystalline sizes of the CFms containing C-coated graphite increased from 2.113 nm to 2.504 nm with increasing amounts of C-coating on the graphite filler.

The CFms containing C-coated graphite were prepared using graphite filler coated with different amounts carbon, and the resulting thermal conductivities and compressive strengths are indicated in Table 2. As a reference material, CFm had a thermal conductivity of 2.35 ± 0.00 W/mK with an apparent density of 0.67 g/cm^3. CFm-C0.5G, CFm-C1.0G, CFm-C2.0G, and CFm-C3.0G had thermal conductivities of 2.00 ± 0.01, 3.40 ± 0.02, 3.37 ± 0.00, and 2.12 ± 0.01 W/mK, respectively, and their apparent densities were 0.40, 0.58, 0.47 and 0.50 g/cm^3, respectively. Jana et al. [23] previously reported that when different graphite particle sizes were used as fillers in CFms, the apparent density decreased with increasing graphite particle size due to the lower surface area determined by interpolation. Therefore, we think that the apparent density reduction was generated by a decreasing number of contacts of the C-coating with the graphite with

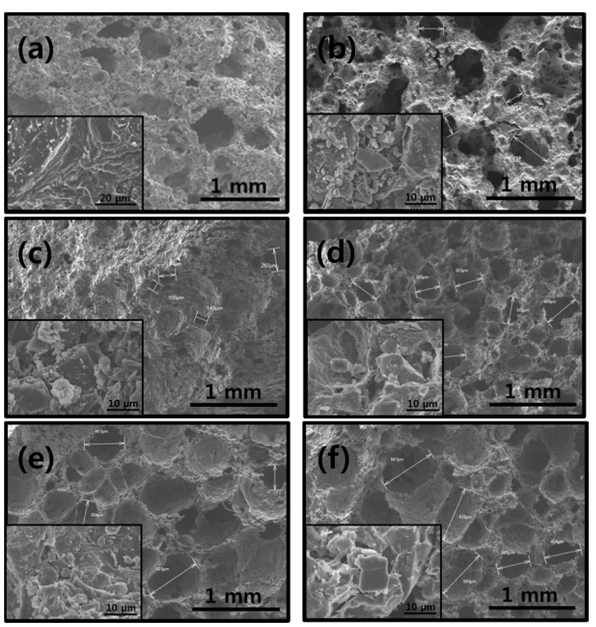

Fig. 3. Surface morphologies of the Carbon foams (CFms) with carbon-coated graphite: (a) CFm, (b) CFm-C0.0G, (c) CFm-C0.5G, (d) CFm-C1.0G, (e) CFm-C2.0G and (f) CFm-C3.0G.

Table 1. I_D/I_G ratios, interlayer spacings and crystalline sizes of the CFms containing C-coated graphite

Sample	I_D/I_G ratio	Interlayer spacing, d_{002} (nm)	Crystalline size, Lc (nm)
CFm	1.03	0.3553	1.701
CFm-C0.0G	0.94	0.3568	2.142
CFm-C0.5G	0.89	0.3558	2.113
CFm-C1.0G	0.93	0.3580	2.125
CFm-C2.0G	0.93	0.3575	2.916
CFm-C3.0G	0.94	0.3581	2.504

I_D/I_G, intensity of D and G band peak, CFms, carbon foams; C-coated, carbon-coated.

Table 2. Compressive strengths and thermal conductivities of the CFms containing C-coated graphite

Sample	Thermal conductivity (W/mK)	Compressive strength (MPa)	True density (g/cm^3)	Apparent density (g/cm^3)
CFm	2.35 ± 0.00	2.30 ± 0.61	1.90	0.67
CFm-C0.5G	2.00 ± 0.01	1.51 ± 0.39	1.79	0.40
CFm-C1.0G	3.40 ± 0.02	4.21 ± 0.11	1.95	0.58
CFm-C2.0G	3.37 ± 0.00	3.83 ± 0.25	1.92	0.47
CFm-C3.0G	2.12 ± 0.01	2.85 ± 0.24	1.92	0.50

Values are presented as mean ± standard deviation.
CFms, carbon foams; C-coated, carbon-coated.

increasing C-coating thickness. However, among the prepared samples, CFm-C1.0G showed the highest thermal conductivity of 3.40 ± 0.02 W/mK because the thermal conductivity was affected by the increased interfacial binding between the CFm and the C-coated graphite due to the low interfacial resistance. The interfacial binding between the CFm and the C-coated graphite was confirmed to be controlled by the amount of C-coating on the graphite filler. The compressive strengths were 2.30 ± 0.61, 1.51 ± 0.39, 4.21 ± 0.11, 3.83 ± 0.25, and 2.85 ± 0.24 MPa for CFm, CFm-C0.5G, CFm-C1.0G, CFm-C2.0G and CFm-C3.0G, respectively. These results were also affected by the interfacial binding between the CFms and the C-coated graphite, as were the thermal conductivity results. Thus, among all the samples, CFm-C1.0G showed the highest compressive strength.

In this study, to improve the structure and properties of CFms, a graphite filler was C-coated using different concentrations of QI-free MP. The I_D/I_G ratios of the CFms containing C-coated graphite decreased and then increased with increasing amounts of C-coating on the graphite filler. The I_D/I_G reduction was attributed to improved interfacial binding between the CFms and the C-coated graphite filler with reduced crystalline defects. Additionally, the crystalline thickness (Lc) of the CFms containing C-coated graphite increased continuously from 2.113 nm to 2.504 nm according to the increasing amount of C-coating on the graphite. The interfacial binding between the CFm and the C-coated graphite was confirmed to be controlled by the amount of C-coating on the graphite filler. Compared with the other CFms, CFm-C1.0G had the highest thermal conductivity and compressive strength, which were 83.03% and 44.68%, respectively. We attributed the increased thermal/mechanical properties to increasing interfacial binding due to reduced interfacial resistance.

Conflict of Interest

No potential conflict of interest relevant to this article was reported.

Acknowledgements

This work was supported by the Defense Acquisition Program Administration and the Agency for Defense Development under the contract UD140046GD.

References

[1] Pranoto I, Leong KC. An experimental study of flow boiling heat transfer from porous foam structures in a channel. Appl Therm Eng, 70, 100 (2014). https://doi.org/10.1016/j.applthermaleng.2014.04.027.

[2] Steinmann WD, Tamme R. Latent heat storage for solar steam systems. J Sol Energy Eng, 130, 011004 (2008). https://doi.org/10.1115/1.2804624.

[3] do Couto Aktay KS, Tamme R, Müller-Steinhagen H. Thermal conductivity of high-temperature multicomponent materials with phase change. Int J Thermophys, 29, 678 (2008). https://doi.org/10.1007/s10765-007-0315-7.

[4] Klett J, Hardy R, Romine E, Walls C, Burchell T. High-thermal-conductivity, mesophase-pitch-derived carbon foams: effect of precursor on structure and properties. Carbon, 38, 953 (2000). https://doi.org/10.1016/S0008-6223(99)00190-6.

[5] Focke WW, Badenhorst H, Ramjee S, Kruger HJ, Schalkwyk RV, Rand B. Graphite foam from pitch and expandable graphite. Carbon, 73, 41 (2014). https://doi.org/10.1016/j.carbon.2014.02.035.

[6] Han YJ, Kim J, Yeo JS, An JC, Hong IP, Nakabayashi K, Miyawaki J, Jung JD, Yoon SH. Coating of graphite anode with coal tar pitch as an effective precursor for enhancing the rate performance in Li-ion batteries: effects of composition and softening points of coal tar pitch. Carbon, 94, 432 (2015). https://doi.org/10.1016/j.carbon.2015.07.030.

[7] Deng T, Zhou X. Porous graphite prepared by molybdenum oxide catalyzed gasification as anode material for lithium ion batteries. Mater Lett, 176, 151 (2016). https://doi.org/10.1016/j.matlet.2016.04.073.

[8] Nada SA, Alshaer WG. Comprehensive parametric study of using carbon foam structures saturated with PCMs in thermal management of electronic systems. Energy Convers Manage, 105, 93 (2015). https://doi.org/10.1016/j.enconman.2015.07.071.

[9] Li Q, Chen L, Ding J, Zhang J, Li X, Zheng K, Zhang X, Tian X. Open-cell phenolic carbon foam and electromagnetic interference shielding properties. Carbon, 104, 90 (2016). https://doi.org/10.1016/j.carbon.2016.03.055.

[10] Kim JH, Lee S, Jeong E, Lee YS. Fabrication and characteristics of mesophase pitch-based graphite foams prepared using PVA-AAc solution. Appl Chem Eng, 26, 706 (2015). https://doi.org/10.14478/ace.2015.1102.

[11] Lee S, Kim JH, Jeong E, Lee YS. The preparation and property of carbon foams from carbon black embedded pitch using PU

template. Korean Chem Eng Res, 54, 268 (2016). https://doi.org/10.9713/kcer.2016.54.2.268.

[12] Kim JH, Lee YS. Characteristics of a high compressive strength graphite foam prepared from pitches using a PVA-AAc solution. J Ind Eng Chem, 30, 127 (2015). https://doi.org/10.1016/j.jiec.2015.05.013.

[13] Ciecierska E, Jurczyk-Kowalska M, Bazarnik P, Gloc M, Kulesza M, Kowalski M, Krauze S, Lewandowska M. Flammability, mechanical properties and structure of rigid polyurethane foams with different types of carbon reinforcing materials. Compos Struct, 140, 67 (2016). https://doi.org/10.1016/j.compstruct.2015.12.022.

[14] Ciecierska E, Jurczyk-Kowalska M, Bazarnik P, Kowalski M, Krauze S, Lewandowska M. The influence of carbon fillers on the thermal properties of polyurethane foam. J Therm Anal Calorim, 123, 283 (2016). https://doi.org/10.1007/s10973-015-4940-2.

[15] Sun Y, Tang B, Huang W, Wang S, Wang Z, Wang X, Zhu Y, Tao C. Preparation of graphene modified epoxy resin with high thermal conductivity by optimizing the morphology of filler. Appl Therm Eng, 103, 892 (2016). https://doi.org/10.1016/j.applthermaleng.2016.05.005.

[16] Gantayat S, Prusty G, Rout DR, Swain SK. Expanded graphite as a filler for epoxy matrix composites to improve their thermal, mechanical and electrical properties. New Carbon Mater, 30, 432 (2015). https://doi.org/10.1016/S1872-5805(15)60200-1.

[17] Narasimman R, Vijayan S, Prabhakaran K. Carbon-carbon composite foams with high specific strength from sucrose and milled carbon fiber. Mater Lett, 144, 46 (2015). https://doi.org/10.1016/j.matlet.2015.01.016.

[18] Rahimi Z, Zinatizadeh AAL, Zinadini S. Preparation of high antibiofouling amino functionalized MWCNTs/PES nanocomposite ultrafiltration membrane for application in membrane bioreactor. J Ind Eng Chem, 29, 366 (2015). https://dx.doi.org/10.1016/j.jiec.2015.04.017.

[19] Farhan S, Wang R, Jiang H, Li K, Wang C. A novel combination of simple foaming and freeze-drying processes for making carbon foam containing multiwalled carbon nanotubes. Ceram Int, 42, 8980 (2016). https://doi.org/10.1016/j.ceramint.2016.01.131.

[20] Lee SE, Lee MY, Lee MK, Jeong E, Lee YS. Effect of fluorination on the mechanical behavior and electromagnetic interference shielding of MWCNT/epoxy composites. Appl Surf Sci, 369, 189 (2016). https://doi.org/10.1016/j.apsusc.2016.01.266.

[21] Chen D, Yang J, Chen G. The physical properties of polyurethane/graphite nanosheets/carbon black foaming conducting nanocomposites. Compos Part A Appl Sci Manuf, 41, 1636 (2010). https://doi.org/10.1016/j.compositesa.2010.07.013.

[22] Yuan Y, Zhang N, Li T, Cao X, Long W. Thermal performance enhancement of palmitic-stearic acid by adding graphene nanoplatelets and expanded graphite for thermal energy storage: a comparative study. Energy, 97, 488 (2016). https://doi.org/10.1016/j.energy.2015.12.115.

[23] Jana P, Fierro V, Pizzi A, Celzard A. Thermal conductivity improvement of composite carbon foams based on tannin-based disordered carbon matrix and graphite fillers. Mater Des, 83, 635 (2015). https://doi.org/10.1016/j.matdes.2015.06.057.

[24] Sengupta R, Bhattacharya M, Bandyopadhyay S, Bhowmick AK. A review on the mechanical and electrical properties of graphite and modified graphite reinforced polymer composites. Prog Polym Sci, 36, 638 (2011). https://dx.doi.org/10.1016/j.progpolymsci.2010.11.003.

[25] Katzman HA. Carbon-reinforced metal-matrix composites. US Patent 4,376,803 (1983).

[26] Lee YS, Kim TJ. Rheological behaviors of mesophase pitches prepared from coal tar pitch as carbon fiber precursor. J Korean Ind Eng Chem, 10, 690 (1999).

[27] Cuesta A, Dhamelincourt P, Laureyns J, Martínez-Alonso A, Tascón JMD. Comparative performance X-ray diffraction and Raman microprobe techniques for the study of carbon materials. J Mater Chem, 8, 2875 (1998). https://doi.org/10.1039/A805841E.